PHYSICAL REVIEW B VOLUME 24, NUMBER 10 15 NOVEMBER 1981

Iron clusters: Electronic structure and magnetism

Chiang Y. Yang* and K. H. Johnson
Department of Materials Science and Engineering, Massachusetts Institute of Technology, Cambridge, Massachusetts 02139

D. R. Salahub and J. Kaspar
Département de Chimie, Université de Montréal, Case Postale 6210, Succursale A, Montréal, Québec H3C 3V1, Canada

R. P. Messmer
General Electric Company, Corporate Research and Development, Schenectady, New York 12301
(Received 15 April 1981; revised manuscript received 19 June 1981)

Self-consistent-field $X\alpha$-scattered-wave molecular-orbital calculations have been performed for iron clusters containing four, nine, and fifteen atoms. The convergence of several properties toward the values for bulk iron has been examined. The dominance of magnetic effects on the electronic structure is quickly established; even the four-atom cluster displays the large exchange splitting and high magnetic moment characteristic of bulk iron. Some other quantities, such as the *d*- and especially the *s*-band width, converge more slowly. For Fe_{15} all of the major features of the bulk density of states (DOS) are present in the cluster DOS. The energy positions of the DOS peaks are sufficiently near those of bulk iron that a qualitative discussion of the binding in bulk iron may be given in terms of the nature of the cluster wave functions. Spin-density maps have been generated for Fe_{15} and these bear a striking resemblance to those derived from neutron scattering experiments on bulk iron. Values of the contact hyperfine field have been calculated and, for the peripheral atoms, reasonable agreement with band theory and with experimental results is found. The experimentally observed increase in the magnetic moment of iron at high temperature is rationalized on the basis of the cluster calculation for Fe_{15}. While one is able to obtain much insight into the properties of bulk iron by examining those of Fe_{15}, there are also some clear differences due to the finite size of the cluster. The central atom has an excess negative charge of about one, and most of this extra charge is of minority spin, leading to a magnetic moment which is much smaller than those for the peripheral atoms. The local density of states at the central atom is also atypical as is the detailed form of the spin density and the value of the contact hyperfine field. Overall the peripheral atoms are more bulklike than the central atom despite the fact that they are missing some nearest neighbors. Non-spin-polarized calculations for Fe_{15} lead to a better understanding of why iron is ferromagnetic through a Stoner-type analysis. For paramagnetic Fe_{15} the Fermi level is situated very near the overall maximum of the DOS. Moreover the cluster wave functions at ϵ_F are antibonding and hence highly localized in space, which would lead to a large value for the cluster "Stoner integral." Thus a rationalization for the instability of paramagnetic iron has been obtained in terms of quantum chemical concepts.

I. INTRODUCTION

The body of knowledge concerning the properties of small aggregates of atoms has advanced to the point that it is appropriate to speak of "cluster science." A cluster may be defined as an aggregate containing at least two atoms and at most the number of atoms required to yield a value of a property which is indistinguishable from that of a bulk sample, within the accuracy of a given experiment. Hence, beyond a certain number of atoms, which will in general be different for each type of

measurement, the addition of further atoms will have a negligible effect on an intensive property of the aggregate. If one considers a cluster which is just large enough to yield the bulk value of a property, then for that particular property, studying the cluster is equivalent to studying a bulk specimen. If the cluster study can be made more easily than a bulk study, or if the theoretical framework necessary to interpret the results is conceptually simpler or computationally more convenient, then it is clearly advantageous to study the cluster. That is, clusters may be, and have been, used as models for the study of bulk phenomena.[1-3] On the other hand, one is often interested, both theoretically and in practical applications, in the properties of clusters in the size range where convergence to the bulk values of properties has not yet been attained. The prime example of this type of interest is in the field of heterogeneous catalysis.[4] The catalytic properties of smooth extended surfaces of a metal can be radically different from those of small particles. In this situation one is interested in the intrinsic properties of a cluster and the emphasis is often placed on differences of these properties, compared with those of the bulk metal or of an infinite surface. Other examples of studies in which cluster properties are examined in their own right may be found in the rapidly developing field of cluster beams.[5] It is now possible to prepare beams of metal clusters having a very narrow size distribution. Experiments are being planned[6] to measure some of the properties of these clusters so that there is now a clear and direct interest in calculations of the properties of clusters *per se*. These are important experiments, not only because some of the properties of the clusters may be interesting and of potential technological utility but also since they will provide unambiguous tests of the various cluster calculations which are being performed.

The majority of the calculations of the electronic structure of metal clusters has been made within the framework of molecular-orbital theory and prominent among these have been studies[1-3] using the self-consistent-field $X\alpha$-scattered-wave method (SCF-$X\alpha$-SW).[7] Calculations on metal clusters using this method have proven to be of value in a variety of contexts and several reviews of these applications exist.[3] Of most relevance to the present paper is the study of Messmer *et al.*[1] on clusters of Cu, Ni, Pd, and Pt containing up to thirteen atoms. It was found that even such small clusters contain much of the essential physics of the bulk metals, for these particular metals and for the properties considered ("low resolution" density of states, photoemission, existence and approximate value of magnetic moments). However, as pointed out in Ref. 1, the small size of the clusters does manifest itself in several ways; for example, there is a large charge imbalance between the central atom and its neighbors.

The thirteen atom clusters considered in Ref. 1 represent the smallest cluster which retains the local symmetry present in the bulk fcc metals. The degree of agreement with bulk properties which was found for Cu_{13}, Ni_{13}, Pd_{13}, and Pt_{13} lends confidence that similar studies of other transition metals should yield a useful level of convergence toward the bulk, and that the information represented by the cluster eigenvalues and wave functions might provide an adequate framework for a local, chemical-bonding interpretation of some of the properties of the transition metals. Compared with band-theoretical treatments, cluster calculations possess several advantages provided that the property under investigation is sufficiently localized that a relatively small cluster yields bulklike results. For clusters in the size range mentioned above a calculation is computationally less demanding than a band calculation. Wave-function and charge-density information is more readily extracted from a cluster calculation and these may yield explanations of solid-state phenomena in terms of quantum chemical concepts providing either new interpretations or at least complementary information to that which may be extracted from band theory. Finally, the (point-group) symmetry conditions imposed on the cluster wave functions are less restrictive than the (space-group) conditions imposed by the periodicity of the solid in a band calculation. This allows the cluster wave functions a certain amount of variational freedom to localize in different parts of the cluster and in some applications this is beneficial or even crucial.

We are currently carrying out an extensive, multifaceted program of calculations on metal clusters containing up to about twenty atoms (and sometimes more). Because of their central importance in several fields (e.g., catalysis, metallurgy, magnetism) our effort is currently focused on the transition metals of the iron series. The entire $3d$ series is being treated in order to evince the systematics. The results of these calculations can serve many purposes and we are examining their possible implications (both as models for bulk metals and in their own right) for (i) the conceptual basis by which the chemical bonding in metals may be un-

derstood, (ii) the understanding of metallic surfaces and chemisorption thereon, (iii) the interpretation of valence and core photoelectron spectra, (iv) understanding of the magnetic properties of the clusters, the bulk metals, and metallic surfaces, including the effects of changes in pressure and temperature and changes of phase, and (v) comprehension of at least certain electronic aspects of the transport properties (conductivity and superconductivity) of metals.

We have to date completed the basic calculations for clusters of all of the 3*d* transition metals except Mn (because of its complicated crystal structure—58 atoms in the unit cell). These clusters contain thirteen atoms for the fcc and hcp metals and fifteen atoms (first and second neighbors) for the bcc cases. This paper is concerned with iron clusters, but before treating this element in detail it is worth establishing perspective by pointing out a few generalities which have so far been gleaned from the series of calculations. The details will be given in forthcoming publications.[8] Overall, the degree of similarity of the cluster results to those of band theory is, as expected, similar to that found for Cu_{13}, Ni_{13}, Pd_{13}, and Pt_{13}. For each element we find a relatively narrow band originating from the *d* orbitals. This is overlapped in all cases by a few levels representative of the broader *s-p* band. There is a reasonable correspondence between the cluster density of states (DOS) and the coarse structure of the DOS from band calculations. The clusters mimic to a very high degree the gross magnetic properties found in the bulk metals. That is, calculations for Sc_{13}, Ti_{13}, V_{15}, and Cu_{13} either converged to a closed-shell configuration or, for those clusters having an odd number of electrons, converged, when spin polarization was allowed, to a state having a single extra majority-spin electron and a negligible exchange splitting of corresponding up-spin and down-spin levels. Hence these clusters may be labeled nonmagnetic in agreement with the behavior observed for the bulk metals. Spin-polarized calculations for Fe_{15}, Co_{13}, and Ni_{13} all exhibit large exchange splittings and appreciable net-spin electron numbers in agreement with the observed ferromagnetism of the bulk metals. The exchange splitting and the magnetic moment are largest for Fe_{15}, intermediate for Co_{13}, and smallest for Ni_{13} in agreement with the results of spin-polarized band calculations.[9] The calculated average net-spin electron numbers per atom are 2.7 for Fe_{15}, 1.6 for Co_{13}, and 0.5 for Ni_{13} which may be compared with experimental bulk values of 2.2, 1.7, and 0.6, respectively. Cr_{15}, as is discussed in detail elsewhere,[8,10] is magnetic and the moments which may be attributed to each of the three shells of atoms in the cluster have the alternation in sign characteristic of an antiferromagnet.

Along with these points of similarity between the cluster results and either experimental results for the bulk metals or the results of band theory, for each of the clusters mentioned above it is possible to isolate a number of differences caused by the finite cluster size. The central atom always has an excess of electrons and in the cases so far examined its local density of states (LDOS) is less similar to that of the bulk metal than are the LDOS for the peripheral atoms. This is contrary to the intuitive notion that the central atom, since it has its full complement of nearest neighbors should be most bulklike. In fact the lack of coordinative saturation for the exterior atoms of the cluster implies that some electrons, which in the bulk metal would be involved in bonding interactions with atoms that are absent in the cluster, are free to migrate to the central atom. Calculations on larger clusters [Cu_{19} (Ref. 1), Al_{19}, Al_{43} (Ref. 2)] indicate that this effect will persist to quite large aggregates. The results for the magnetic properties of the 3*d* clusters also reveal that there is an imbalance in the spin density between the various atoms of the clusters; all of the atoms do not have the same magnetic moments. This will be discussed in detail below for Fe and in forthcoming publications for the other elements.

The above brief sketch of some of the cluster results is indicative that useful information about the electronic structure and magnetic behavior of the transition metals can be extracted from cluster calcuations. In the remainder of the paper we will consider in detail the results for iron clusters and quantify some of the above discussion.

Because of its high natural abundance, iron is the workhorse of metallurgy and probably the single most important metal technologically. It is also the prototype of itinerant ferromagnets and explanations of its magnetic behavior have been sought for centuries[11] and are still being sought. In particulate form iron is used as a catalyst for many industrially important reactions[12] including the synthesis of ammonia from nitrogen and hydrogen (Haber process) and of high molecular weight paraffins from carbon monoxide and hydrogen (Fischer-Tropsch process). In biology small iron-sulfur clusters form the active centers of the nitrogen fixation enzymes, and ferredoxins.[13] In the

recording industry, particles of iron form the basis of the pigments used in the latest generation of magnetic tapes.[14] There is therefore a clear need for a better understanding of the properties of iron in its various states of aggregation.

A complete account of the properties of iron must include, or even be dominated by, a discussion of magnetic properties. Indeed the chemical properties of iron such as its catalytic activity cannot be divorced from its magnetic properties since the ferromagnetism leads to shifts in the energy levels due to the spin polarization which are of the order of an eV or more. These changes in "orbital electronegativity" relative to the paramagnetic case have profound effects on the interactions between an iron particle or surface and the admolecules of interest in catalytic processes.[15] A complete quantitative treatment of the finite temperature magnetic behavior of the transition metals does not presently exist, although considerable progress has been made in recent years.[16] The magnets of the iron series have proven to be particularly problematic since the $3d$ electrons are neither completely localized onto single centers nor entirely delocalized. Indeed, both the localized Heisenberg picture in which an individual magnetic moment is assigned to each atom and these are allowed to interact through an effective exchange parameter J, and the itinerant electron theory developed by Stoner and implemented in connection with modern band theory have been invoked to explain different aspects of the magnetic behavior of iron, cobalt, and nickel. Band theory appears to be adequate for the ground-state, zero temperature magnetic properties. For instance, spin-polarized band calculations[9,17] for Fe, Co, and Ni yield values for the magnetic moments in good agreement with experiment. The spin splitting obtained for Fe and Co is in quite good agreement with that deduced from angle-resolved photoemission spectra.[18] Some discrepancies do exist, however, for Ni and are the subject of intense current debate.[19]

Severe problems arise if one wishes to extend the itinerant electron model in a straightforward manner to finite temperature and the approach breaks down entirely for the paramagnetic regime above the Curie point. In Stoner theory[20–22] the exchange splitting is proportional to the magnetization, so that at T_c both the splitting and the magnetic moments disappear. This approach leads to calculated values of the Curie temperature which are an order of magnitude too high and it also leads to disagreement with neutron scattering results[23] which indicate the existence of spin-wave-like excitations and hence, of local moments well above the Curie temperature. Photoemission experiments[24] below and above the Curie point show that the exchange splitting persists in the paramagnetic regime and a recent theoretical interpretation[25] maintains that an appropriately defined exchange splitting does not have any important temperature dependence near T_c. Thus between T_c and about $1.4T_c$ it appears that iron is not a "normal" itinerant paramagnet, lacking local moments, but rather that the moments persist and exhibit short-range order, the net zero magnetization of a bulk sample being due to a lack of long-range order. A basic problem with Stoner theory, or finite-temperature band theory is one of symmetry. Since all of the atoms must have the same moment, the only way to obtain a zero magnetization for the sample within this theory is to destroy all of the moments, or equivalently to remove the exchange splitting. Since this requires, for iron, an energy of about 1.5 eV (15 000 K) the calculated "Curie temperature" is far too high. The more modern theories of magnetism for the transition metals either directly or implicity allow the translational symmetry of the lattice to be broken. The emphasis has shifted to considerations of short-range order rather than the long-range order necessarily present in a band calculation.

"Itinerant" magnetism is coming to be viewed more and more as a localized phenomenon, where the localization is not strictly at the atomic level but rather over a relatively small number of atoms. One is dealing with essentially a molecular-type problem rather than either an atomic one or a highly delocalized itinerant electron problem. We believe that ultimately a real-space cluster-type approach would be useful in understanding magnetism at finite temperatures, although the small clusters considered below are clearly inadequate for the quantitative treatment of any phenomena whose range is larger than the cluster diameter (about 5 Å) and the calculations are for zero temperature. Nevertheless, as we will argue below, some insight into certain effects of temperature can be gained by considering the possible effects of excitations from occupied to empty cluster orbitals.

In the following sections we present results of SCF-$X\alpha$-SW calculations, both non-spin-polarized and spin-polarized, for iron clusters containing four, nine, and fifteen atoms. The electronic and magnetic structure of the clusters will be compared and contrasted with that yielded by band theory

for bulk iron and where possible with experimental results. Preliminary accounts of some of the calculations have already appeared.[10,15,26]

II. MODELS, METHODS, AND PARAMETERS

The structures of the Fe_4, Fe_9, and Fe_{15} clusters are depicted in Fig. 1. Fe_9 and Fe_{15} correspond to fragments of a bcc lattice and the normal bulk nearest-neighbor spacing of 2.49 Å has been used. The second-neighbor distance is 2.87 Å. The tetrahedral Fe_4 cluster does not correspond to part of the bcc lattice; nevertheless we include it here as an example of a very small cluster in order to obtain a better idea of the rate of convergence of the various properties toward their bulk values and also to give some indication of the sensitivity of the various results to structural changes. The Fe-Fe distance was again chosen to be 2.49 Å.

The calculations were performed with the self-consistent-field $X\alpha$-scattered-wave molecular-orbital method which is well documented elsewhere.[7] The results in the next section have been obtained with tangent spheres and include partial waves up to $l=2$ in the atomic spheres and up to $l=4$ in the outer-sphere region. The exchange parameter α was taken from the compilation of Schwarz[27] and is equal to 0.711 51. There has been some discussion in the literature[17,21,28] about whether the $X\alpha$ form for the local exchange-correlation functional is well suited for the quantitative treatment of magnetic systems and, if so, what value of α should be used. The recommended values[27] of α appear to yield overestimates of the exchange splittings and magnetic moments. In recent linear combination of atomic orbitals (LCAO) band calculations, Callaway and Wang[17] found that the von Barth–Hedin[29] functional gave somewhat better agreement for the moments; however, the Kohn-Sham[30] potential ($X\alpha$ with $\alpha=\frac{2}{3}$)

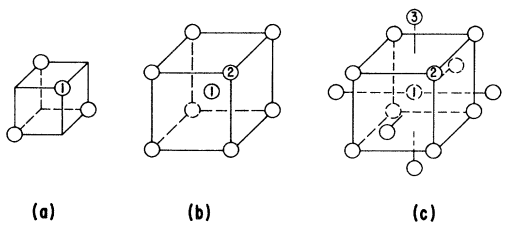

FIG. 1. Structure of the clusters (a) Fe_4, (b) Fe_9, (c) Fe_{15}. The numbers refer to groups of symmetry-related atoms.

yielded somewhat better values for the hyperfine field. Since there is no concensus we have preferred to retain the approach which has been used in past cluster studies and is currently in wide use for molecules, namely the $X\alpha$ potential with the Schwarz values of α. Future work will be aimed at examining the sensitivity of the results to changes in the form of the potential; however, since the $X\alpha$ calculations predict the correct type of magnetism for the different $3d$ metals, it would appear that the errors caused by the $X\alpha$ approximation are of a quantitative nature (and reasonably small) rather than qualitative ones.

It has often been found in molecular $X\alpha$-SW calculations[31] that improved eigenvalues and spectroscopic results can be obtained by allowing the spheres which define the muffin-tin potential to expand and overlap one another. The possible effects of allowing overlapping spheres in the more close-packed case of clusters representing bulk metals have not heretofore been examined. While intuition would suggest that a strict nonoverlapping muffin-tin treatment should be more appropriate for the globular clusters considered here than for the more open structures often observed in molecules, the question of the effects of overlapping spheres does arise. We have therefore carried out some test calculations in which sphere overlap was permitted and these will be compared here with the tangent sphere results in order not to disrupt the continuity of the next section.

In Fig. 2 we show the energy levels calculated for the Fe_4 cluster with (a) touching spheres, (b) sphere radii increased by 15%, and (c) sphere radii increased by 30%. The lowest a_1 level of case (b) and a number of levels of case (c) yielded small negative electron populations for the intersphere region and, as is usually done in overlapping-sphere calculations, these were reset to zero and the wave functions were renormalized. This behavior indicates that a 30% increase in sphere radii is near the maximum which the method will allow before overlap errors dominate the numerics. The gross features of the electronic structure of Fe_4 are not overly sensitive to the value of the sphere radii. The ordering of the energy levels is similar in all cases with only a few interchanges of close-lying levels. All three calculations show a large exchange polarization and high net-spin electron numbers of 2.5 for the touching-sphere case and 3.0 for both overlapping-sphere cases, the difference being caused by the transfer of one electron from the $3t_2^{\downarrow}$ orbital to $4t_2^{\uparrow}$ when the spheres overlap.

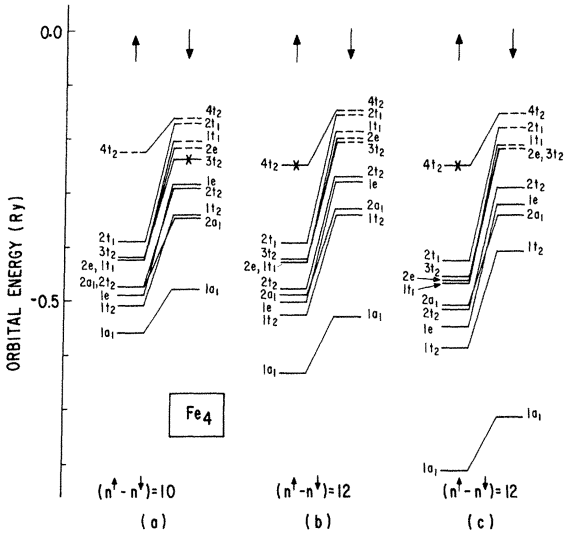

FIG. 2. Orbital eigenvalues from spin-polarized calculations for Fe_4. (a) Touching spheres, (b) 15% increase in sphere radii, (c) 30% increase of sphere radii. The Fermi level is shown by an $\times$ representing the single electron which occupies it.

All calculations yield a narrow d band delimited by the $1t_2$ and $2t_1$ levels, overlapped by levels of higher s-p character which are representative of the wide s-p band found for bulk iron. The width of the d band increases somewhat upon overlap, being 0.12, 0.14, and 0.16 Ry for the majority spin levels of (a), (b), and (c), respectively. By far the most sensitive levels are the lowest ones of each spin, $1a_1$, which move progressively to lower energy as the sphere radii are increased.

Since in what follows we will be highly concerned with magnetic properties we have examined the effect of overlapping spheres on the spin density of Fe_4. Plots of the spin density, the difference in the densities of majority- and minority-spin electrons, are shown in Fig. 3 for a plane containing two iron atoms and bisecting the line between the remaining two atoms of the tetrahedron. Figure 3(a) is from the tangent-sphere calculation while Fig. 3(b) is for the 30% increase in sphere radii. Again, while there are quantitative differences, the two calculations yield qualitatively similar results, namely a dense region of positive spin density surrounding the nuclei and a more diffuse region of reverse polarization between the atoms and in the interstitial region. Similar plots for Fe_{15} will be discussed in detail in the next section.

As a final example of the effects of overlapping spheres we show, in Fig. 4, the orbital eigenvalues

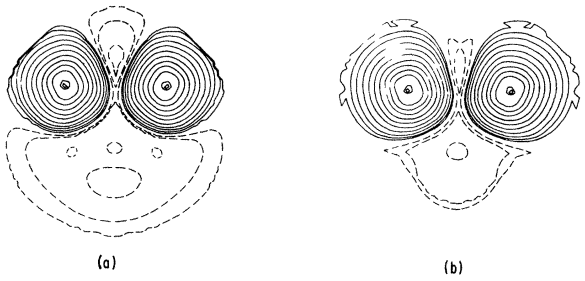

FIG. 3. Contour map of the spin density $[\rho\uparrow(\vec{r}) - \rho\downarrow(\vec{r})]$ for Fe_4 in a plane containing two nuclei and bisecting the line joining the other two nuclei. (a) Touching spheres, (b) 30% increase of sphere radii. Dashed lines indicate negative values. The lowest contour shown has the value 0.001 a.u. and adjacent contours differ by a factor of 2.

from non-spin-polarized calculations for Fe_{15} using (a) touching spheres and (b) radii increased by 20%. Once again, for the 20% overlap case a few of the levels have been renormalized to remove negative intersphere-electron populations. The vast majority of the eigenvalues undergo an approximately constant upward shift of about 0.15 Ry

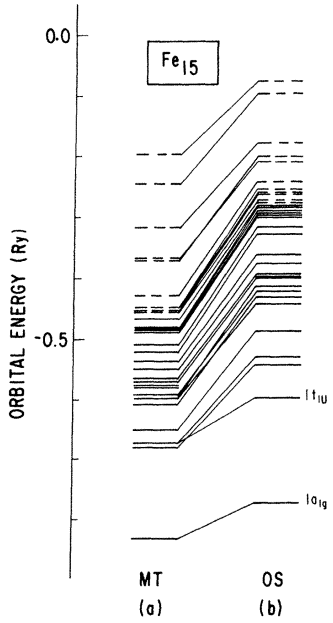

FIG. 4. Orbital eigenvalues from non-spin-polarized calculations for Fe_{15} (a) touching spheres, (b) sphere radii increased by 15%. Unoccupied levels are indicated by dashed lines. See also Fig. 12.

when the sphere radii are increased. There are some interchanges of close-lying levels. The two most atypical levels are $1a_{1g}$ and $1t_{1u}$ both of which have high contributions from s and p partial waves. As in the case of Fe_4, the major effect of overlapping spheres is to move these levels to lower energy relative to the d band.

In summary, the overlapping-sphere calculations indicate that the general features, at a semiquantitative level, of the electronic structure of metal clusters are relatively insensitive to reasonable amounts of overlap and in what follows we will discuss only results from tangent-sphere calculations.

It should be pointed out here that for the case of Fe_{15} there are some small differences in the energy-level spectrum compared with that given in preliminary accounts.[15,26] These differences arise for the following reasons. The calculations reported in the next section were made with a finer numerical integration grid than was used in the earlier work and this can cause small changes in the eigenvalues. For cases like Fe_{15} where the density of levels is very high around the Fermi level, these small changes can modify the occupancy of some levels, which because of the self-consistent nature of the calculation causes further changes in the eigenvalues. In the $X\alpha$ method the Fermi statistics are formally satisfied. In practice, however, it is not always possible to attain convergence using integral occupation numbers and strict observance of the Fermi statistics. One either has to adjust fractional occupation numbers so that all of the partially occupied levels have a common energy, which defines the Fermi level, or to allow the Fermi statistics to be relaxed to a certain extent. The practical consequence is that one can achieve a reasonable degree of convergence for electronic configurations which differ for one or a few electrons. To be specific, for the Fe_{15} cluster reported below, the two highest occupied orbitals are partially occupied. They are the $6e_g^{\uparrow}$ level which contains one electron and has an eigenvalue of -0.4117 Ry and the $4t_{1u}^{\downarrow}$ level which contains two electrons and has an eigenvalue of -0.4119 Ry. In the earlier calculations the $6e_g^{\uparrow}$ level was empty and the positions of the eigenvalues were slightly different from those reported in Ref. 10 and below. The effects of these changes on the properties of Fe_{15} are relatively minor. For example, the average net-spin electron number per atom which was previously reported as 2.53 is found to be 2.67 in the more recent calculations.

III. RESULTS AND DISCUSSION

A. Convergence towards the bulk

The molecular-orbital energy eigenvalues from spin-polarized calculations for Fe_4 have already been presented in Fig. 2. Those for Fe_9 and Fe_{15} are shown in Figs. 5 and 6, respectively. The values of a number of key quantities are summarized in Table I where they are compared with results from band theory and with experimental values for bulk iron. Comparing Figs. 2, 5, and 6, and associated information on the wave functions, one is at first struck by the qualitative similarities among the three clusters and also by the high degree of overall resemblance to the results of band theory (see Refs. 9 and 17). The effects of spin-polarization are predominant for all of the clusters as well as for bulk iron. All of the clusters are ferromagnetic and one can recognize the precursors of the bulk iron majority- and minority-spin d and sp bands. For the d bands the exchange splitting, $\Delta\epsilon_x$ between corresponding majority- and minority-spin levels (see Table I and Figs. 2, 5, and 6), is of the same order of magnitude as that of band theory. The exchange splitting appears to be a very localized property and is not very sensitive to cluster size. As in band theory $\Delta\epsilon_x$ is not constant over the d manifold indicating that "rigid-band" arguments should be viewed with caution. Smaller values of $\Delta\epsilon_x$ are found near the bottom of the d band and the largest values are near the middle. Staying with the d band, we also show in Table I the positions relative to the Fermi level for the bottom of the d band (i.e., the width of the occupied part) and estimates of the total d-band widths. The occupied d-band width increases steadily on going from Fe_4 to Fe_9 to Fe_{15}; this property is more sensitive to cluster size than was the exchange splitting. For the largest cluster, Fe_{15}, we obtain, for majority and minority spin, respectively, about 94% and 85% of the bulk occupied bandwidths as obtained from band theory.

There is some ambiguity in defining the top of the d band in the cluster results (as there also is in band theory because of hybridization) the source of which is best seen by comparing the energy level spectra for Fe_9 and Fe_{15}. In the majority-spin manifold of Fe_9, the levels of predominantly d character, are delimited by $1e_g^{\uparrow}$ (-0.60 Ry) and $4t_{1u}^{\uparrow}$ (-0.42 Ry). There is then a large gap of about 0.2 Ry until the unoccupied $4e_g^{\uparrow}$ level which has high contributions from s and p as well as d

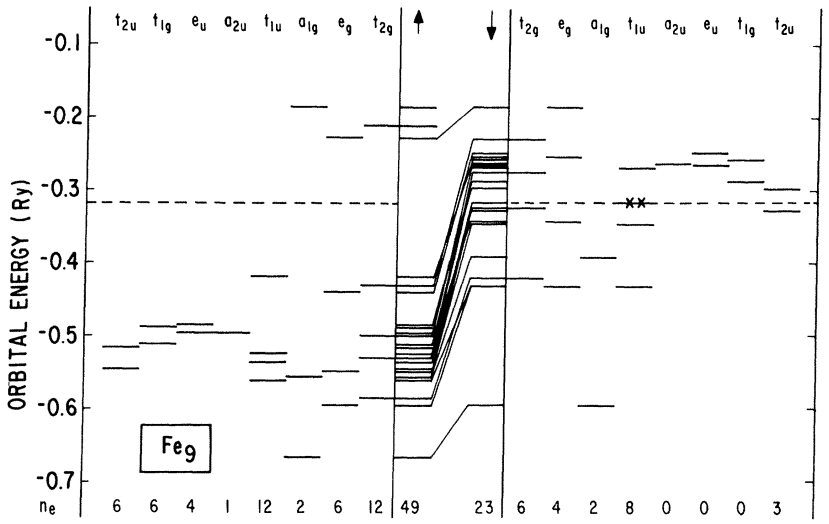

FIG. 5. Orbital eigenvalues from the spin-polarized calculation for Fe_9. The dashed line indicates the position of the Fermi level, $3t_{1u}^{\downarrow}$ which is occupied by two electrons. The bottom line shows the number of electrons of each spin and symmetry type (point group O_h) as well as the total number of majority- and minority-spin electrons.

partial waves. The presence of this gap is clearly a cluster effect; in the band calculations there are majority-spin states between the Fermi level and a large spike in the DOS (see below) which occurs near -1 eV, although the DOS is quite small in this region. A major difference between Fe_9 and Fe_{15} is that this gap is greatly reduced in the latter. In fact the analogs of the $4e_g^{\uparrow}$ and the close-lying $5t_{2g}^{\uparrow}$ levels of Fe_9 are the $6e_g^{\uparrow}$ and $7t_{2g}^{\uparrow}$ levels of Fe_{15} which lie just at ϵ_F. These correspond to highly

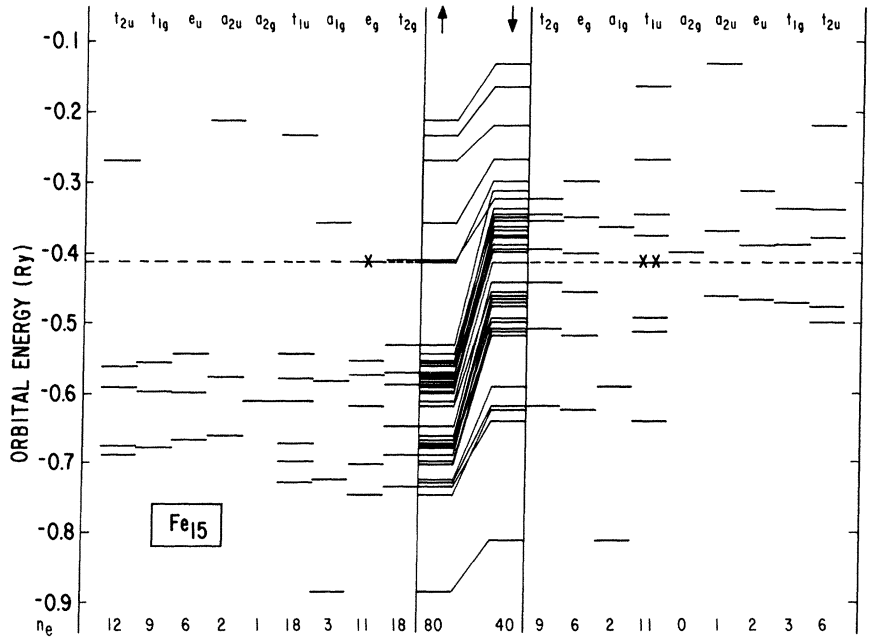

FIG. 6. Orbital eigenvalues from the spin-polarized calculation for Fe_{15}. The dashed line indicates the position of the Fermi level, which is coincident with the $6e_g^{\uparrow}$ (one electron) and $4t_{1g}^{\downarrow}$ (two electrons) levels. The bottom line shows the number of electrons of each spin and symmetry type (point group O_h) as well as the total number of majority- and minority-spin electrons.

TABLE I. Comparison of properties of iron clusters with those of bulk iron.[a]

	Fe_4	Fe_9	Fe_{15}	Band theory[c]	Expt.
$[(n\uparrow - n\downarrow)/N]$[b]	2.5,[d] 3.0[e]	2.9	2.7	2.30[f]	2.12[g]
Bottom of s band ($\uparrow$)	4.4[h]	4.7[h]	6.2[h]	8.2[i]	9.2[j]
($\downarrow$)	3.3[h]	3.7[h]	5.4[h]	8.1[i]	
Bottom of d band ($\uparrow$)	3.7[k]	3.8[l]	4.5[l]	4.8[m]	4.6[n]
($\downarrow$)	1.5[k]	1.5[l]	2.9[l]	3.4[m]	
Width of d band ($\uparrow$)	1.6[o]	2.4[p]	2.9,[q] 4.5[r]	5.1[s]	
($\downarrow$)	2.3[o]	2.8[t]	4.3,[u] 4.5[v]	6.4[s]	
Range of exchange splitting (d)	1.7–3.0	1.8–3.2	1.2–3.2	1.6–2.7	1.5[w]
Average exchange splitting (d)	2.6	2.7	2.5		
Exchange splitting (sp)	1.1[x]	1.0[y]	0.8[y]	0.2[z]	

[a] Energies are in eV.
[b] Average net-spin electron number per atom.
[c] Reference 17, values quoted are for Kohn-Sham ($\alpha=\frac{2}{3}$) potential.
[d] Tangent spheres, see text.
[e] Overlapping spheres, see text.
[f] The von Barth–Hedin potential yields 2.16.
[g] Reference 32 including a g factor of 2.09.
[h] $\epsilon_F-\epsilon(1a_1)$.
[i] $\epsilon_F-\epsilon(\Gamma_1)$.
[j] Reference 33—some uncertainty may exist because of difficulties in locating point of intersection of the spectrum with base line.
[k] $\epsilon_F-\epsilon(1t_2)$.
[l] $\epsilon_F-\epsilon(1e_g)$.
[m] $\epsilon_F-\epsilon(N_1)$.
[n] Ultraviolet photoelectron spectroscopy, polycrystalline, Ref. 34. Angle-resolved studies for Fe(111) (Ref. 18) also yield reasonable agreement with band theory for the width of the occupied d bands at the symmetry point P.
[o] $\epsilon(2t_1)-\epsilon(1t_2)$.
[p] $\epsilon(4t_{1u})-\epsilon(1e_g)$.
[q] $\epsilon(6t_{2g})-\epsilon(1e_g)$.
[r] $\epsilon(7t_{2g})-\epsilon(1e_g)$.
[s] $\epsilon(N_3)-\epsilon(N_1)$.
[t] $\epsilon(4t_{2g})-\epsilon(1e_g)$.
[u] $\epsilon(3e_u)-\epsilon(1e_g)$.
[v] $\epsilon(6e_g)-\epsilon(1e_g)$.
[w] From angle-resolved photoemission Ref. 18 . The value is for the P point. Band theory yields an exchange splitting at this point of 1.3 eV for the von Barth–Hedin potential and 1.6 eV for the Kohn-Sham potential.
[x] $\epsilon(1a_1^{\downarrow})-\epsilon(1a_1^{\uparrow})$.
[y] $\epsilon(1a_{1g}^{\downarrow})-\epsilon(1a_{1g}^{\downarrow})$.
[z] $\epsilon(\Gamma_1^{\downarrow})-\epsilon(\Gamma_1^{\uparrow})$.

hybridized dsp orbitals and represent to a certain extent the majority-spin bands in the vicinity of the Fermi energy. The gap is reduced from 0.2 Ry for Fe_9 to about 0.14 Ry for Fe_{15}. If more atoms were added to the cluster this gap would eventually be occupied by further energy levels representing this portion of the band structure in more detail. Hence it is not completely clear whether the top of the majority-spin cluster d band should be defined as the energy of the $6t_{2g}^{\uparrow}$ level or as that of $7t_{2g}^{\uparrow}$. Values for both choices are included in Table I. The former choice has the advantage of emphasizing the fact that for the closely spaced d manifolds (between $1e_g^{\uparrow}$ and $6t_{2g}^{\uparrow}$ and between $1t_{1u}^{\downarrow}$ and $6e_g^{\downarrow}$) the dispersion is significantly greater for minority spin in agreement with band theory, while the latter choice more nearly represents the spread in energy over which significant contributions from d partial waves are found. In this case one obtains about 88% and 70% of the total bulk bandwidths

for majority and minority spins, respectively. total bulk bandwidths for majority and minority spins, respectively.

Cluster levels which are precursors of the broad *sp* band which overlaps and hybridizes with the *d* band can also be identified. These are rather few and widely spaced so that convergence to a good representation of the bulk is much slower for the more delocalized *sp* states. The easiest of these levels to isolate is the lowest totally symmetric one (a_1 under T_d and a_{1g} under O_h symmetry) which lies at considerably lower energy than the predominantly *d* levels. There is only this single cluster energy level in each spin to represent the *sp* band over the energy range between the bottom of the *d* band and the bottom of the *s* band, i.e., a range of more than 3 eV. Clearly any property of bulk iron which depends on a good representation of the energy states in this region will be rather poorly represented by a 15-atom cluster. The spin polarization of the lowest a_{1g} level is smaller than that for the *d* levels but much larger than that found at the bottom of the *s* band for bulk iron. The difference in energy between the $1a_{1g}$ level and the bottom of the *d* band increases steadily as the number of atoms in the cluster increases and at the same time $\Delta\epsilon_x$ decreases. Fe_{15} yields, respectively, about 75% and 67% of the occupied majority- and minority-spin *s* band widths of bulk iron. Since the $1a_{1g}$ levels are the lowest valence levels of the clusters and the bottom of the *s* band at Γ represents the lowest valence level in a band calculation there is natural tendency to identify $1a_{1g}$ with Γ_1. While the analogy is strong it is not perfect because of the different symmetry constraints on the wave functions in the two cases. In a band calculation including functions up to $l=2$, the wave function for Γ_1 is a Bloch wave composed entirely of *s* functions. The a_{1g} cluster orbitals are also restricted to *s* functions for the central atom; however, appropriate linear combinations of *p* and *d* functions on the off-center atoms can be constructed which transform as a_{1g} and the cluster $1a_{1g}$ levels do contain non-negligible contributions from *p* and *d* waves. For example, the ratio of *s*:*p*:*d* character averaged over all 15 atomic spheres for the $1a_{1g}$ level of Fe_{15} is 7.1:1:1.3. Hence, from the points of view of its energy position, its spin splitting, and the characteristics of the wave function, the $1a_{1g}$ level resembles more closely band states which are somewhat removed from the Γ point, allowing *spd* hybridization.

The final property related to the convergence of the series of clusters shown in Table I is the average net-spin electron number per atom. This quantity, like $\Delta\epsilon_x$ to which it is related, is reasonably converged even for the smallest cluster, Fe_4. The values are somewhat higher than either those calculated from band theory [with a smaller value of $\alpha(=\frac{2}{3})$ or with the von Barth–Hedin potential] or the experimental value.

Table I and the above discussion indicate that Fe_{15} represents a reasonably converged model for the gross features of the electronic and magnetic structure of bulk iron. The existence of ferromagnetism, the value of the magnetic moment, that of the exchange splitting, the positions and widths of the precursors of the majority and minority *d* and *s* bands are all in sufficient agreement with the corresponding quantities for the bulk, that a qualitative discussion of the electronic structure of bulk iron based on the calculations for Fe_{15} is justified. We proceed now to give such a discussion and also to further delineate the quantitative differences between Fe_{15} and bulk iron.

B. DOS of Fe_{15} and of bulk iron

In Fig. 7 we present the DOS for majority and minority spin generated from the Fe_{15} calculation by replacing each energy level by a Gaussian of width parameter 0.2 eV. Figure 8 shows the DOS from a recent band calculation for ferromagnetic iron.[9] For the majority-spin DOS of Fe_{15} we obtain five peaks, labeled 1–5, below ϵ_F, which may be associated with the features labeled 1–5 for the bulk DOS. The cluster and the band DOS show a reasonable degree of correspondence. As mentioned above, the low-lying tail of the DOS corresponding to the bottom part of the *sp* band is represented by a single cluster energy level which gives rise to peak 1. There is structure in both the cluster and the bulk *d*-band DOS, the most prominent features of which are three peaks which increase in magnitude as one goes from lower to higher energy. The approximate centers of these peaks are at −4.6, −3.2, and −1.0 eV for bulk iron and at −4.3, −3.6, and −2.3 eV for Fe_{15}. Thus, relative to bulk iron, peaks 2 and 3 for Fe_{15} are at about the right energy but somewhat too close to each other and peak 4 is about an eV too low. At the Fermi level both the cluster and the band calculation indicate a moderate majority-spin DOS. The large separation between peaks 4 and 5 for the cluster is the most noticeable difference between the cluster and the band DOS. For minority

spin the peaks labeled 6—9 are the most prominent features of both the cluster and the bulk DOS. Again the relative magnitude and disposition of the peaks is quite similar in the two calculations. Both calculations indicate that the majority- and minority-spin DOS are not simply shifted mirror images of one another, i.e., that there are significant departures from the rigid-band model.

The centers of peaks 7—9 are at approximately -3.0, -1.4, and $+1.6$ eV for the band calculation and at -3.0, -1.0, and $+0.7$ eV for the cluster. The increased width of the valley between peaks 7 and 8 of the band DOS compared with that between the corresponding majority-spin peaks 2 and 3 is also present in the cluster DOS. The Fermi level of the band calculation is situated at the bottom of the valley between peaks 8 and 9; for the cluster ϵ_F is about 0.3 eV above the bottom of the valley and the down-spin DOS is relatively higher than that predicted by band theory. Recent spin-polarized photoemission experiments for iron[35] yielded a positive polarization of 60% at threshold which decreased, but remained positive, with increasing photon energy to reach an asymptotic value of about 15% for photon energies above 8 eV. This behavior is consistent with the band DOS; at ϵ_F majority spin predominates and if one

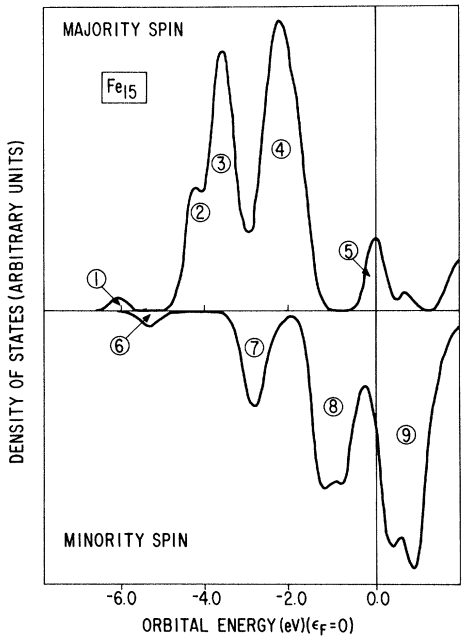

FIG. 7. Majority- and minority-spin densities of state for Fe_{15}. The curves were generated by replacing each discrete cluster eigenvalue with a Gaussian of width parameter 0.2 eV.

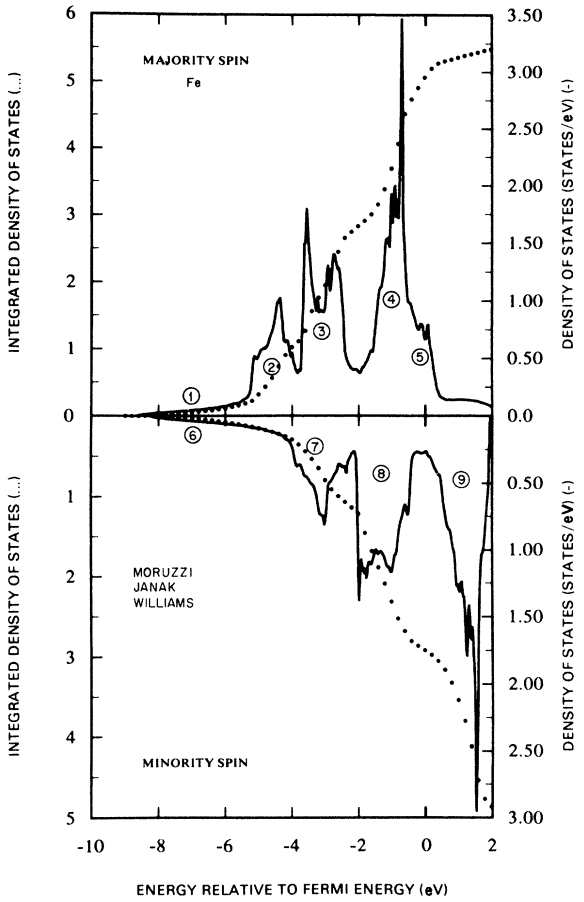

FIG. 8. Majority- and minority-spin densities of state for bcc iron. From Moruzzi, Janak, and Williams (Ref. 9).

simply integrates the DOS for each spin downwards from ϵ_F, it is clear from Fig. 8 that for all energies there will be excess majority spin. For Fe_{15}, on the other hand, we would predict a negative spin polarization for energies between ϵ_F and about $\epsilon_F - 2$ eV. Hence, for this particular property, Fe_{15} is an inadequate model for bulk iron. It would clearly be interesting, if one could make a beam of Fe_{15} clusters (and if the structure was not too different from the bulklike geometry treated here) to perform spin-polarized photoemission experiments to verify whether this feature, which distinguishes Fe_{15} from bulk iron, can, in fact, be observed. It appears that such experiments are within the realm of possibility and we hope they will be attempted.

One of the major advantages of the cluster approach is that the wave functions corresponding to the various energy levels can be readily generated and examination of these can yield deeper insight

into the nature of the bonding. We turn now to a discussion of the various peaks in the cluster DOS (and by analogy in the band DOS) in terms of the nature of the orbitals which contribute to them. In general the wave functions for corresponding levels in the up- and down-spin manifolds are not radically different and also essentially similar to those from the non-spin-polarized calculation. The most noticeable differences occur for a few pairs of levels ($4e_g$, $5e_g$; $4t_{2g}$, $5t_{2g}$; $5t_{1u}$, $6t_{1u}$) which lie close in energy. The wave functions for up- and down-spin levels within these pairs do not bear a one-to-one correspondence to each other. For example, the spatial part of the $4e_g^{\uparrow}$ wave function corresponds to a combination of $4e_g^{\downarrow}$ and $5e_g^{\downarrow}$ rather than simply to $4e_g^{\downarrow}$. Apart from such mixing the only systematic difference which is apparent from examination of the wave functions is that for orbitals involving bonding interactions the minority-spin levels are slightly more diffuse than their majority-spin counterparts as is illustrated for a typical case in Fig. 9. In an LCAO sense this would correspond to larger overlaps between atomic orbitals centered on neighboring atoms and is consistent with the larger width of the minority-spin d band compared with that of majority spin.

Peaks 1 and 6 in the cluster DOS (Fig. 7) correspond to a single orbital $1a_{1g}$ which is a bonding linear combination of a 4s orbital on the central atom and *sdp* hybrids on the peripheral atoms. Based on a partial-wave analysis of the charge within the muffin-tin spheres, there is about 80% s, 10% p, and 10% d character. Peaks 2 and 7 each result from four energy levels, $1e_g$, $1t_{2g}$, $1t_{1u}$, and $2a_{1g}$, which are all bonding molecular orbitals. $1e_g$ and $1t_{2g}$ involve d orbitals almost exclusively, whereas $1t_{1u}$ and $2a_{1g}$ also have non-negligible contributions from s and p functions. A total of ten energy levels contribute to each of the peaks 3 and 8. The associated orbitals still have a high degree of bonding character but less than those associated with the lower-energy peaks 2 and 7. Bonding interactions involving d electrons on the central atom are either absent by symmetry or weak (except for the t_{2g} orbitals) so that the predominant interactions for most of these orbitals involve the atoms on the periphery of the cluster. Hence, some of the bonding interactions are between second-nearest neighbors and would be consequently weaker. For many of the orbitals of this group there exist antibonding interactions between some of the atoms which also reduce the overall bonding character of the orbital. For the eighteen orbitals which give rise to peaks 4 and 9 the degree of bonding is much less and as one proceeds through the orbitals contributing to this peak from low energy to high, antibonding interactions become progressively more dominant. Finally, at still higher energy one observes peak 5 which is due to the $6e_g$ and $7t_{2g}$ orbitals, which are strongly antibonding mixtures of d functions on the central atom with

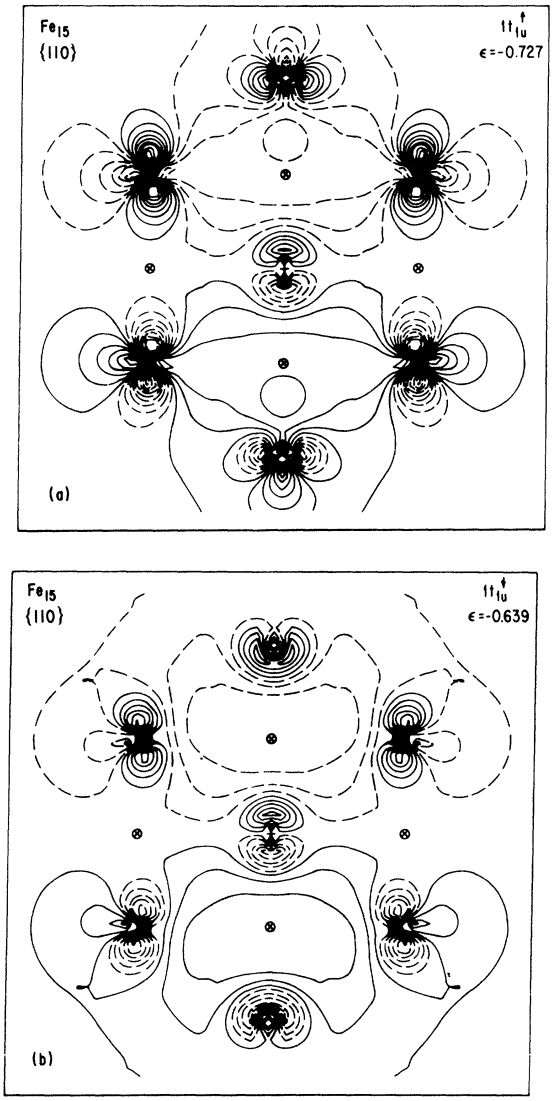

FIG. 9. Contour maps of the (a) $1t_{1u}^{\uparrow}$ and (b) $1t_{1u}^{\downarrow}$ wave functions from the spin-polarized calculation for Fe_{15}. The plane shown is a {110} plane passing through atoms 1, 2, and 3 of Fig. 1. Dashed lines represent negative values of the wave function. The lowest contour has the value 0.01 a.u. and adjacent contours differ by 0.02 a.u. Nuclei lying above the plane are represented by an $\times$ and those below the plane by an $\circ$.

spd hybrid functions on the peripheral atoms. Hence, all of the major features of the DOS can be characterized in quantum chemical terms and there is a natural progression from bonding, predominantly *s* orbitals (peaks 1 and 6) to bonding *d* orbitals (peaks 2 and 7) to essentially nonbonding (or weakly bonding or weakly antibonding) *d* functions (peaks 3 and 8), to antibonding *d* states (peaks 4 and 9), and finally to antibonding levels involving both *d* and *s* functions (peak 5).

C. Spin density

The degree to which Fe_{15} represents a good model for bulk iron can be further quantified by a comparison of the spin or magnetization density for the cluster with that deduced from neutron scattering experiments.[36] Such a comparison is made in Fig. 10 for a (100) plane which contains second-nearest neighbors [four atoms of type 2 (see Fig. 1)]. The experimentally derived magnetization density of iron is characterized by nearly, but not quite, spherical regions of very high positive magnetization (up to 500 kG) centered at the nuclei which account for most of the magnetic moments. There are, however, large regions of small (up to 2 kG) negative magnetization which are approximately in the shape of interlocking tori centered at the midpoint of the line joining second neighbors and perpendicular to that line. One of these toroidal shaped regions is depicted in Fig. 10(a). The regions of positive magnetization (the four sets of concentric circles) are represented schematically[36] rather than realistically in order to emphasize the regions of negative magnetization. The most negative values are found at the intersections of the tori and are denoted by the open triangles in Fig. 10(a). The corresponding map generated from the Fe_{15} wave functions is shown in Fig. 10(b). There is a remarkable degree of similarity to the experimental data. Each iron atom in Fig. 10(b) is surrounded by a region of high positive spin density and in the middle of the square one observes a region of negative spin density of the same general form as that observed experimentally. The most negative values are at about the same positions as in Fig. 10(a). Hence, the qualitative features of the magnetization density of bulk iron are well represented by the spin density for these peripheral atoms of Fe_{15}. On a quantitative level the maximum positive field calculated for the cluster is about 380 kG and the largest negative field is about -1 kG which may be compared to the values of 500 and -2 kG for bulk iron. It is clear from Fig. 10(b) that the positive magnetization regions for Fe_{15} are not spherical; however, since these are peripheral atoms the inherent anisotropy

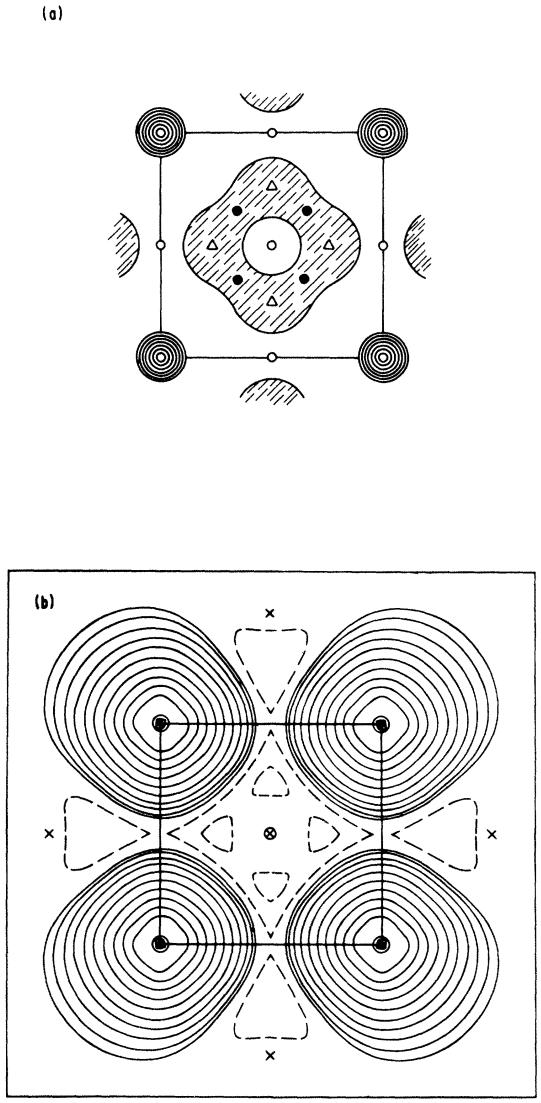

FIG. 10. (a) Representation of the magnetization density for bulk iron in a {100} plane measured by neutron scattering. Adapted from Ref. 36. The positive (circular) contours have been drawn schematically in order to emphasize the (hatched) region of negative polarization. The symbols represent the following values of the magnetic field: ○, $+1.0\pm0.3$ kG; ●, -1.0 ± 0.3 kG; Δ, -2.0 ± 0.4 kG. (b) Contour map of the spin density for Fe_{15} plotted in a {100} plane containing four atoms of type 2 (see Fig. 1). Dashed lines represent negative values of the spin density. The lowest contour has the value 0.001 a.u. (0.524 kG) and adjacent contours differ by a factor of 2.

due to the lack of some neighbors prevents us from making any conclusions about the small observed anisotropy.

D. Finite temperature

Continuing with the magnetic properties we will now comment on certain temperature effects which in the past have posed severe problems to the existing theories of magnetism. Some of these can be given a simple explanation in terms of the calculation for Fe_{15} if one assumes that the only effect of a finite temperature is to excite some of the electrons from occupied to vacant levels.

Molecular-field theory has been successfully applied to explain the magnetic behavior of transition metals, either from the point of view of localized electrons (Weiss model) or itinerant electrons (Stoner model). However, one major deficiency of the molecular-field theory is its inability to explain the apparent difference in the magneton number below and above the Curie temperature. The effective magneton number for iron below T_c deduced from magnetization measurements is 2.22 (2.11 electrons) and that above T_c deduced from susceptibility versus $1/T$ measurements is 3.2 (3.06 electrons). It will be shown below that the $X\alpha$ cluster model furnishes a simple explanation for these observations.

First, it is important to mention the neutron diffraction studies on iron at $T > T_c$ by Shull *et al.*[36–38] and by Spooner and Averbach.[23] Two significant conclusions among others are the following. (a) The small-angle scattering results indicate the existence of spin clusters above T_c. In other words, short-range ordering of the spins persists well into the paramagnetic region. For example, at 80 °C above T_c, clusters of atoms with spin correlation are found and the typical size is about 10 Å or 45 atoms. (b) The diffuse scattering results indicate that, up to a temperature of about 1000 °C (γ phase), the paramagnetic moment is approximately $2.7\mu_B$, which is 25% greater than the moment at low temperature.

There is, therefore, good reason to think that the electronic structure of iron in the paramagnetic region might be more appropriately described by a cluster model. For the Fe_{15} cluster, it is clear from Fig. 6 that the lowest-lying excitations would involve transfer of electrons from the minority-spin levels just below ϵ_F to the $6e_g^{\uparrow}$ and $7t_{2g}^{\uparrow}$ levels. Such excitations would lead to an increase of the magnetic moment. For the case of full excitation, four electrons would be transferred to the majority spin (1 for $6e_g$, three for $7t_{2g}$) and the resultant effective ferromagnetic electron number would be 3.2 (or $3.34\mu_B$). On the other hand, if the excitation is less complete, a smaller value of n_e would be expected. There is reasonable agreement with the value of $3.2\mu_B$ from susceptibility measurements above T_c and $2.7\mu_B$ from neutron diffraction measurements in the vicinity of T_c, respectively. Hence, the cluster model yields a perfectly natural explanation for these experimental results whereas either a local moment or a completely itinerant theory is incapable of so doing. The difficulty of the (local) Weiss model arises from the assumption that electrons separate out onto particular atoms and each atom has a fixed magnetic moment; therefore, there is no mechanism for changing the moment as temperature increases. For the itinerant Stoner model, although the inconsistency of the magneton number is less apparent, the shortcomings of this model are fundamentally more serious, when it is applied to the paramagnetic region. First of all, the disappearance of spontaneous magnetization at $T > T_c$ in the band theory incorrectly implies zero averaged magnetic moment per atom. Furthermore, since the magnetic moments vanish in this theory, so does the exchange splitting and, as mentioned above, this is inconsistent with the results of photoemission studies.

E. Intrinsic cluster properties

In the above discussion we have dealt with a number of properties of iron and have pointed out that the cluster model, and especially Fe_{15}, can furnish conceptually simple, real-space interpretations of many of these properties at the semiquantitative level. We also pointed out in passing a few differences between the results for Fe_{15} and those for bulk iron. We will now turn to a more detailed discussion of the intrinsic properties of the cluster. Indeed clusters would be much less interesting both from academic and technological points of view if they were simply miniaturized versions of the bulk material. The most prominent differences occur in properties which may be attributed to the various atoms of the cluster. In Fe_{15} there are three different types of atoms (see Fig. 1) and each is in a different environment, whereas in a perfect, infinite, periodic crystal of iron all atoms are equivalent. Most of the properties discussed above were presented in terms of average values for the cluster as

a whole. In Table II we present some properties of Fe_{15} which can be analyzed on an atom-by-atom basis. As usual in $X\alpha$-SW calculations there is no unique way to apportion the charge or spin density in the intersphere (II) and extra-molecular (III) volumes among the atoms so we give a separate entry for regions II and III. It is clear from Table II that the charge distribution in Fe_{15} is not uniform; the central atom has about one electron more than either of the peripheral atoms. Furthermore, this "extra" electron is predominantly of minority spin so that the magnetic moment associated with the central atom is much smaller than those of the peripheral atoms. The decrease in the magnetic moment is mainly due to differences in the *d*-electron distribution; however there are also non-negligible contributions from *s* and *p* functions. Overall, as shown by the local configurations given in Table II, the central atom has a slightly higher *s* character and a significantly higher *p* character than the peripheral atom. Values for the spin density at the three different iron nuclei (the contact hyperfine field) are also given in Table II. The total field has been broken down into contributions from the individual core levels and a valence contribution. Comparing with the results of band theory and experiment one observes that for this property also there is better agreement for the peripheral atoms both for the total field and also for the relative sizes of the various contributions. For the peripheral atoms, the qualitative picture of the source of the hyperfine field deduced from the cluster calculation is similar to that derived from band theory.[17,40] The largest contributions come from core polarization with a small negative field arising from the 1*s* shell, a large negative field from 2*s*, and a partially compensating large positive field for the 3*s* shell. The valence contribution is relatively small and of opposite sign for the nearest and second-nearest neighbors. This change of sign is also present in the net contribution of *s*-type spin density to the net spin-electron numbers shown in Table II. The central atom is quite different; here the largest overall contribution comes from the valence shell, consistent with the relatively large (compared to the other two types of atoms) *s* contribution of -0.05 to the net spin electron number. To maintain perspective it should be stated that the hyperfine field is very sensitive to the details of the electron distribution. For example, Callaway

TABLE II. Analysis of some properties of the Fe_{15} cluster.

		Fe[a](1)	Fe(2)	Fe(3)	II + III[b]
Number of valence electrons					
	total	8.04	6.97	6.83	15.21
	s	0.48	0.35	0.36	
	p	0.46	0.18	0.12	
	d	7.11	6.44	6.35	
Configuration[c]		$d^{7.0}s^{0.5}p^{0.5}$	$d^{7.4}s^{0.4}p^{0.2}$	$d^{7.45}s^{0.4}p^{0.15}$	
$n\uparrow - n\downarrow$	total	1.15	2.70	2.81	0.37
	s	-0.05	-0.01	0.00	
	p	-0.06	0.00	0.00	
	d	1.26	2.71	2.80	
Spin density at nucleus					Band theory[e]
	1*s*	-0.01 (-10)[d]	-0.05 (-24)	-0.05 (-25)	-0.13 (-68)
	2*s*	-0.56 (-292)	-1.27 (-664)	-1.29 (-675)	-0.86 (-450)
	3*s*	$+0.33$ ($+170$)	$+0.65$ ($+335$)	$+0.65$ ($+341$)	$+0.53$ ($+278$)
	valence	-0.79 (-415)	-0.10 (-53)	$+0.14$ ($+74$)	-0.20 (-105)
	total	-1.05 (-547)	-0.77 (-406)	-0.55 (-286)	-0.66 (-346)
	expt. total	-0.65 (-339)[f]			

[a] See Fig. 1 for numbering of atoms.
[b] Intersphere plus outersphere.
[c] Normalized to eight electrons.
[d] Values in parentheses are contact hyperfine field in kG.
[e] Reference 17, Kohn-Sham potential.
[f] Reference 39.

and Wang[17] found a difference of over 50% between the values calculated with the Kohn-Sham and with the von Barth—Hedin potentials.

Hence, for Fe_{15} as well as for other clusters in this size range, the peripheral atoms are more bulklike than the central atom as is further illustrated in Fig. 11 which shows local density of states curves for each of the three types of atoms. These have been generated in a similar fashion to the DOS curves discussed above except that here the Gaussians for each level are weighted with the charge inside the appropriate muffin-tin sphere. It is clear that the local DOS curves for the peripheral atoms bear a much closer resemblance to the bulk DOS than does that for the central atom. For example in the latter case the peak at −3.6 eV (peak 3 in the cluster DOS) is very weak and the lower-lying peak (peak 2) is much more intense than in the bulk DOS. Both of these results indicate that there is more weight relative to the bulk for the highly bonding orbitals of Fe_{15} involving the central atom. This would suggest that a real Fe_{15} cluster might have internuclear separations which are smaller than the bulk lattice spacing.

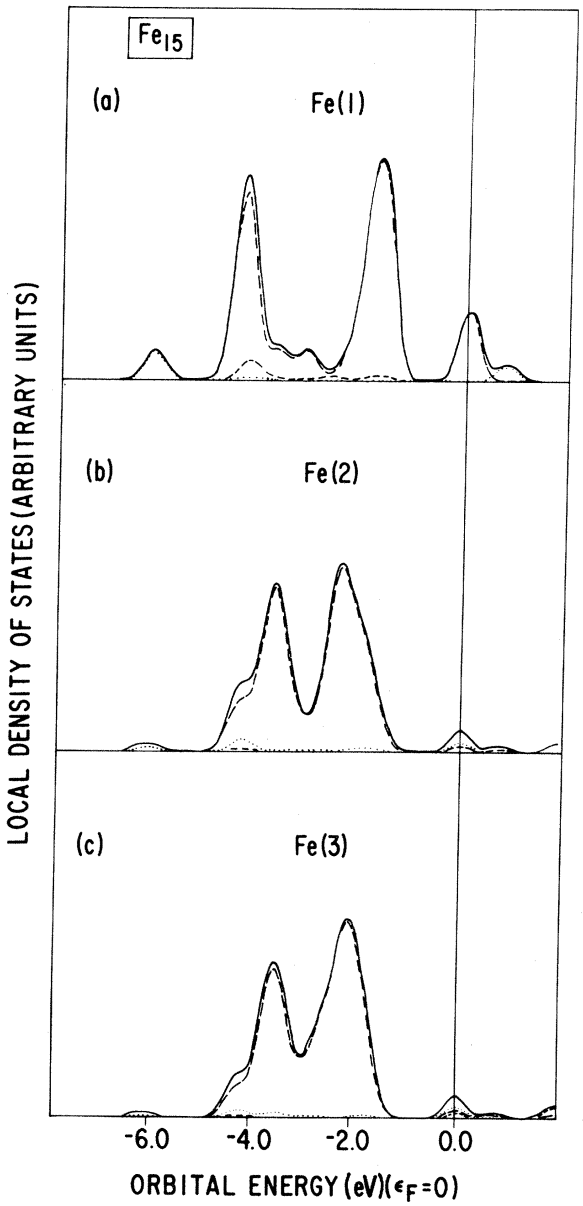

FIG. 11. Local densities of states (majority spin) for the three different types of atoms of the Fe_{15} cluster. See Fig. 1 for atom numbering. Generated by replacing each discrete cluster eigenvalue with a Gaussian of width parameter 0.2 eV weighted with the charge contained within the appropriate muffin-tin sphere. —— total, · · · *s* contribution, - - - *p* contribution, — — — *d* contribution.

F. Paramagnetic calculations—Stoner criterion

The final results which we wish to present are derived from non-spin-polarized calculations for Fe_{15}. Since magnetic (or superconducting) metals depart from the "normal" paramagnetic state it would clearly be informative if one could isolate the feature(s) of the electronic structure of the paramagnetic metal which are the cause of its instability. This is one of our goals in performing the cluster calculations for the entire 3*d* series. The clusters we have considered are sufficiently reliable models for the bulk metals that the occurrence or absence and the general features of magnetic ordering are correctly given by the spin-polarized calculations. The non-spin-polarized calculations provide at least partial answers to such questions as why iron, cobalt, and nickel are ferromagnetic, and the other metals are not. There is ample precedent for this type of study in the Stoner theory of ferromagnetism and its more modern offspring and our analysis will be in this spirit. While the Stoner theory is not a complete theory of magnetism (its failings at finite T were pointed out above) it has been emminently successful in rationalizing the occurence of ferromagnetism among the transition metals. The Stoner theory has been much discussed in the literature and we do not intend to repeat that discussion here. A particularly insightful presentation in the context of modern band theory has been given by Gunnarsson.[21] Janak[22] has done relevant calculations for the elements of the third and fourth rows of the Periodic Table.

The basic idea of Stoner theory is to examine whether the introduction of a net magnetization and its concommittant exchange splitting will result in a higher or lower energy than that of the paramagnetic state. Creating a net magnetization implies that some electrons are transferred from down-spin levels to up-spin levels. This costs band energy but yields a stabilization owing to the increased number of exchange interactions so that a competition is set up and the ground state will be either nonmagnetic or magnetic depending on which term dominates. Following Gunnarsson, the band splitting for band k_n, $\Delta\epsilon_{kn}$ is given by

$$\Delta\epsilon_{kn} = -I(\epsilon_{kn})\Delta m, \tag{1}$$

where Δm is the net magnetization and $I(\epsilon_{kn})$ is a generalized Stoner parameter. Using the von Barth–Hedin functional and making the justified assumption that spherically symmetric contributions from d electrons dominate the problem, I is given by

$$I(\epsilon) = -\int_o^{r_{WS}} r^2 dr \left[\frac{\mu^x(r_s)}{6\pi}\right]\delta(r_s) \times \frac{\phi_2^2(r,\epsilon)\phi_2^2(r,\epsilon_F)}{\rho(r)}, \tag{2}$$

where $r_s = (3/4\pi)^{1/3}\rho^{-1/3}$, $\mu^x = -2/(\pi\alpha r_s)$, $\alpha = (4/9\pi)^{1/3}$, $\delta(r_s) = 1 - 0.036r_s - 1.36r_s/(1+10r_s)$, ρ is the electron density, $\phi_2(r,\epsilon)$ and $\phi_2(r,\epsilon_F)$ are the radial d wave functions for energy ϵ and ϵ_F, respectively, and the integral is over the Wigner-Seitz cell. $\delta(r_s)$ is a parameter which for small spin polarization determines the splitting of up- and down-spin potentials. In this limit, the $X\alpha$ form for the exchange correlation potential corresponds to a density-independent value of δ of $\frac{3}{2}\alpha$. The Stoner criterion for the occurrence of ferromagnetism is that

$$I(\epsilon_F)N(\epsilon_F) > 1\ . \tag{3}$$

Both $I(\epsilon_F)$ and $N(\epsilon_F)$ can be evaluated from paramagnetic band calculations as has been successfully done, for example, by Gunnarsson and by Janak. In a cluster model, because of the discrete nature of the spectrum, one cannot precisely define $I(\epsilon_F)$ and $N(\epsilon_F)$ so that it would be rather difficult to formulate a numerical criterion such as Eq. (3). One can, however, construct DOS curves such as those in Fig. 7 and observe for a particular metal whether or not the paramagnetic Fermi level is situated in a region of high DOS. Comparisons among different metals can also be made. Examination of the wave functions for levels at or near the cluster Fermi energy can also lead to a better understanding of why the cluster equivalent of $I(\epsilon_F)$ is large for some metals and small for others.

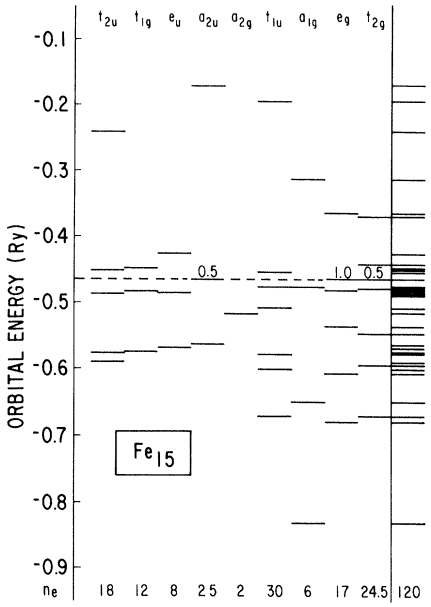

FIG. 12. Orbital eigenvalues from the non-spin-polarized calculation for Fe_{15}. The dashed line indicates the position of the Fermi level which is coincident with the $2a_{2u}$ (0.5 electron), $5e_g$ (1 electron), and $5t_{2g}$ (0.5 electrons) levels. The bottom line shows the number of electrons of each symmetry type (point group O_h).

The calculated eigenvalue spectrum for non-spin-polarized Fe_{15} is shown in Fig. 12. It should be noted that convergence to a configuration satis-

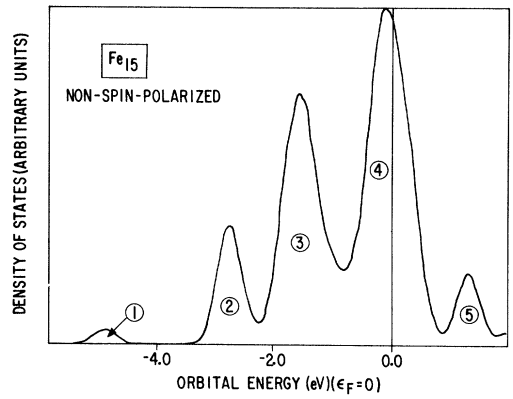

FIG. 13. Density of states from the non-spin-polarized calculation for Fe_{15}. The curve was generated by replacing each discrete cluster eigenvalue with a Gaussian of width parameter 0.2 eV.

fying the Fermi statistics could not be obtained using integral occupation numbers so that the cluster Fermi energy is defined by three partially occupied quasidegenerate levels, $2a_{2u}$, $5e_g$, and $5t_{2g}$ which contain 0.5, 1.0, and 0.5 electrons, respectively. This is a result of the relatively large number of eigenvalues near ϵ_F and already provides some indication that electron spin flips should be obtainable with relatively small increases in kinetic energy. The DOS generated from these levels is shown in Fig. 13. The overall structure is quite similar to those already discussed for ferromagnetic Fe_{15} (Fig. 7) if allowance is made for differential shifts in the peaks due to spin-polarization of the order of an eV or so. The important point for our present purposes is that the Fermi level is very near the absolute maximum in the DOS so that one of the ingredients $N(\epsilon_F)$ of the Stoner criterion, Eq. (3), is large. The fact that $I(\epsilon_F)$ is also large can be better understood by examining the wave functions for the $2a_{2u}$, $5e_g$, and $5t_{2g}$ levels (and also for other close-lying levels). Some representative plots are shown in Fig. 14. These orbitals are all highly antibonding and hence more strongly localized than are bonding orbitals. (Assuming the node is at a bond midpoint, then an antibonding orbital is zero there, whereas a corresponding bonding orbital has some finite value. If the two functions are properly normalized then the antibonding function must take on higher values than the bonding function over much of the atomic volume. Hence it is more strongly peaked, or viewed another way, more rapidly varying in accord with its higher kinetic energy.) To understand why relatively sharply peaked functions should lead to larger values of the Stoner parameter we again follow Gunnarsson. One can evaluate Eq. 2 for $\epsilon=\epsilon_F$ and after some variable changes the following equation is obtained:

$$I(\epsilon_F)=\frac{4}{9\pi\alpha}r_{WS}\int_0^1\left[\frac{r_s}{r}\right]^2\delta(r_s)\Phi^4(r,\epsilon_F)d\left[\frac{r}{r_{WS}}\right], \tag{4}$$

where $\Phi(r,\epsilon_F)=r\phi_2(r,\epsilon_F)$. One can consider the integral in (4) as a weighted average of the function $(r_s/r)^2\,\delta(r_s)\Phi^2(r,\epsilon_F)$ with the normalized weighting function, $\Phi^2(r,\epsilon_F)$. A detailed analysis[21] shows that Φ varies more strongly than the other functions. If Φ has a strong peak then those regions of r near the peak will receive high weights in the integral. But the remaining part of the integrand also contains a term Φ^2 which is large near the

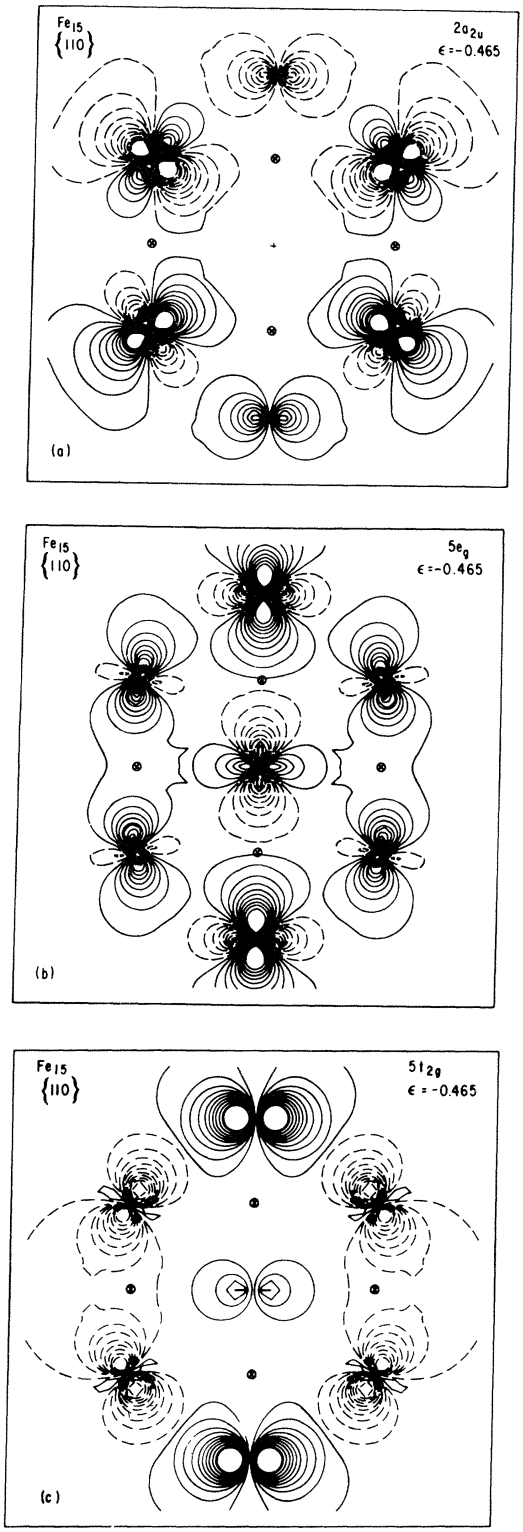

FIG. 14. Contour maps of the (a) $2a_{2u}$, (b) $5e_g$, and (c) $5t_{2g}$ wave functions from the non-spin-polarized calculation for Fe_{15} illustrating the antibonding character of the levels near ϵ_F. See Fig. 9 for details.

peak so that one will weight more heavily the larger values of $(r_s/r)^2\ \delta(r_s)\Phi^2(r,\epsilon_F)$. Hence overall, wave functions which are relatively localized in some region of space will tend to yield large values of I, which is consistent with the intuitive idea that exchange interactions are greater for electrons which are constrained to be closer to each other.

From the above, one can state quite simply that the basic feature of a paramagnetic metal which determines that it possesses a ferromagnetic instability is the presence of a high density of antibonding states at the Fermi level. Paramagnetic Fe_{15}, like bulk paramagnetic iron has this feature.

IV. SUMMARY

The principal conclusions of this work may be summarized as follows.

(1) The gross features of the electronic and magnetic structure of even very small iron clusters are essentially similar to those of bulk iron. Fe_4, Fe_9, and Fe_{15} all show the large exchange splittings and magnetic moment characteristic of the bulk.

(2) Other quantities such as the widths of the d and sp bands and some other details of the density of states converge more slowly so that for a more detailed discussion of the properties of bulk iron, Fe_{15} is a significantly better model than the smaller clusters.

(3) A detailed comparison of the electronic structure of Fe_{15} with that of bulk iron has been made. All of the major features of the bulk density of states are present at approximately the same energies for Fe_{15}.

(4) The major peaks in the DOS may be assigned to orbitals of different chemical bonding types. In order of increasing energy these are (i) bonding, predominately sp orbitals, (ii) bonding d orbitals, (iii) essentially nonbonding d functions, (iv) antibonding d functions, and (v) antibonding levels involving s and p as well as d orbitals.

(5) Spin-density maps for some peripheral atoms of Fe_{15} are in essential agreement with those derived from neutron scattering.

(6) The experimental observation that the magnetic moments increase above the Curie temperature has been rationalized in terms of thermal excitations from cluster orbitals of minority spin to those of majority spin.

(7) The peripheral atoms of Fe_{15} have hyperfine fields which are in reasonable agreement with those calculated from band theory and also with experiment. The contributions from individual core levels and from the valence shell are also consistent with calculations for bulk iron.

(8) While Fe_{15} is a useful model for several properties of bulk iron it also possesses some interesting intrinsic cluster properties. Most of these arise from the different environments of the central atom and the peripheral atoms which yield somewhat different values for those properties which may be assigned to individual atoms. These include the charge, the magnetic moment, the hyperfine field, and the local density of states.

(9) Non-spin-polarized calculations for Fe_{15} have yielded a rationalization in the spirit of the Stoner theory, for the ferromagnetic instability of paramagnetic iron. A qualitative "Stoner criterion" for a cluster may be formulated in the statement that ferromagnetism should occur for those paramagnetic clusters which have a high density of antibonding states at the Fermi level. Similar non-spin-polarized calculations for other para- , ferro- , and antiferromagnetic metals should yield a deeper insight into why certain metals are magnetic and others are not.

ACKNOWLEDGMENTS

One of the authors (D.R.S.) is grateful to the Natural Sciences and Engineering Research Council of Canada and to the General Electric Company for financial support.

*Present Address: Department of Energy and Environment, Brookhaven National Laboratory, Upton, New York 11973.

[1]R. P. Messmer, S. K. Knudson, K. H. Johnson, J. B. Diamond, and C. Y. Yang, Phys. Rev. B 13, 1396 (1976) and references therein.

[2]D. R. Salahub and R. P. Messmer, Phys. Rev. B 16, 2526 (1977) and references therein.

[3]For reviews see, e.g., R. P. Messmer, Surf. Sci. 106, 225 (1981); K. H. Johnson, Crit. Rev. Solid State Mater. Sci. 7, 101 (1978); R. P. Messmer, in *Nature of the Surface Chemical Bond,* edited by T. N. Rhodin and G. Ertl (North-Holland, Amsterdam, 1978); A. B. B. Kunz, in *Theory of Chemisorption,* edited by J. R. Smith (Springer, Berlin, 1980).

[4]See, e.g., E. L. Meutterties, T. N. Rhodin, E. Band, C.

F. Brucker, and W. R. Pretzer, Chem. Rev. 79, 91 (1979); E. L. Meutterties, Bull. Soc. Chim. Belg. 84, 959 (1975); *The Physical Basis for Heterogeneous Catalysis,* edited by E. Drauglis and R. I. Jaffee (Plenum, New York, 1975).

[5]A. Hermann, E. Schumacher, and L. Wöste. J. Chem. Phys. 68, 2327 (1978); W. D. Knight, R. Monot, E. R. Dietz, and A. R. George, Phys. Rev. Lett. 40, 1324 (1978); K. Sattler, J. Muhlbach, and E. Recknagel, *ibid.* 45, 821 (1980).

[6]K. Sattler (personal communication).

[7]J. C. Slater, Adv. Quantum Chem. 6, 1 (1972); *The Self-Consistent Field for Molecules and Solids* (McGraw-Hill, New York, 1974), Vol. 4; K. H. Johnson, Adv. Quantum Chem. 7, 143 (1973).

[8]D. R. Salahub, R. P. Messmer, J. Kaspar, B. N. McMaster, and V. H. Smith, Jr. (unpublished).

[9]V. L. Moruzzi, J. F. Janak, and A. R. Williams, *Calculated Electronic Properties of Metals* (Pergamon, New York, 1978).

[10]D. R. Salahub and R. P. Messmer, Surf. Sci., 106, 415 (1981).

[11]W. Gilbert, *De Magnete* (1600), (translated by Gilbert Club, London, 1900), rev. ed., (Basic, New York, 1958), and references therein.

[12]G. C. Bond, *Catalysis by Metals* (Academic, New York, 1962); J. E. Germain, *Catalytic Conversion of Hydrocarbons* (Academic, New York, 1969).

[13]W. H. Orme-Johnson, Annu. Rev. Biochem. 43, 814 (1974); *Iron-Sulfur Proteins,* edited by W. Lovenbery (Academic, New York, 1976).

[14]K. Bittler and W. Ostertag, Angew. Chem. Int. Ed. Engl. 19, 190 (1980).

[15]C. Y. Yang, Ph.D. thesis, MIT, Cambridge, Mass., 1977; K. H. Johnson, Crit. Rev. Solid State Mater. Sci. 7, 101 (1978).

[16]V. Korenman, J. L. Murray, and R. E. Prange, Phys. Rev. B 16, 4032 (1977); 16, 4048 (1977); 16, 4058 (1977); J. Hubbard, *ibid.* 19, 2626 (1979); 20, 4584 (1979); T. Moriya, J. Magn. Magn. Mater. 14, 1 (1979); M. V. You, V. Heine, A. J. Holden, and P. J. Lin-Chung, Phys. Rev. Lett. 44, 1282 (1980); H. Capellmann, Solid State Commun. 30, 7 (1979); Z. Phys. B 35, 269 (1979), J. Phys. F 4, 1466 (1974).

[17]J. Callaway and C. S. Wang, Phys. Rev. B 16, 2095 (1977); C. S. Wang and J. Callaway, *ibid.* 15, 298 (1977).

[18]D. E. Eastman, F. J. Himpsel, and J. A. Knapp, Phys. Rev. Lett. 44, 95 (1980).

[19]See, e.g., W. Eberhardt and E. W. Plummer, Phys. Rev. B 22, 6470 (1980); L. Kleinman, *ibid.* 22, 6468 (1980) 22, 647 (1980); G. Treglia, F. Ducastelle, and D. Spanjaard, *ibid.* 22, 6472 (1980), and references therein.

[20]E. C. Stoner, Proc. R. Soc. London, Ser. A 154, 656 (1936); 169, 339 (1939).

[21]O. Gunnarsson, J. Phys. F 6, 587 (1976).

[22]J. F. Janak, Phys. Rev. B 16, 255 (1977).

[23]S. Spooner and B. L. Averbach, Phys. Rev. 142, 291 (1966); J. W. Lynn, Phys. Rev. B 11, 2624 (1975); P. C. Riedi, Physica (Utrecht) 91B, 43 (1977).

[24]D. E. Eastman, F. J. Himpsel, and J. A. Knapp, Phys. Rev. Lett. 40, 1514 (1978).

[25]V. Korenman and R. E. Prange, Phys. Rev. Lett. 44, 1291 (1980).

[26]K. H. Johnson, C. Y. Yang, D. Vvedensky, R. P. Messmer, and D. R. Salahub, in *Interfacial Segregation,* edited by W. C. Johnson and J. M. Blakely (American Society for Metals, Cleveland, Ohio, 1979).

[27]K. Schwarz, Phys. Rev. B 5, 2466 (1972).

[28]S. Wakoh and J. Yamashita, J. Phys. Soc. Jpn. 21, 1712 (1966).

[29]U. von Barth and L. Hedin J. Phys. C 5, 1629 (1972).

[30]W. Kohn and L. J. Sham, Phys. Rev. 140, A1133 (1965).

[31]E. g., F. Herman, A. R. Williams, and K. H. Johnson, J. Chem. Phys. 61, 3508 (1974); D. R. Salahub, R. P. Messmer, and K. H. Johnson, Mol. Phys. 31, 529 (1976); D. R. Salahub, A. E. Foti, and V. H. Smith, Jr., J. Am. Chem. Soc. 100, 7847 (1978); J. G. Norman, J. Chem. Phys. 61, 4630 (1974).

[32]H. Danan, A. Herr, and A. J. P. Meyer, J. Appl. Phys. 39, 669 (1968).

[33]L. Ley, O. B. Dabbousi, S. P. Kowalczyk, F. R. McFeely, and D. A. Shirley, Phys. Rev. B 16, 5374 (1977).

[34]L. G. Petersson, R. Melander, D. P. Spears, and S. B. M. Hagstrom, Phys. Rev. B 14, 4177 (1976).

[35]W. Eib and B. Reihl, Phys. Rev. Lett. 40, 1674 (1978).

[36]C. G. Shull and H. A. Mook, Phys. Rev. Lett. 16, 184 (1966).

[37]M. K. Wilkinson and C. G. Shull, Phys. Rev. 103, 516 (1956).

[38]A. A. Gersch, C. G. Shull, and M. K. Wilkinson, Phys. Rev. 103, 525 (1956).

[39]J. I. Budnick, L. J. Bruner, R. J. Blume, and E. L. Boyd. J. Appl. Phys. 32, 120S (1961).

[40]J. F. Janak, Phys. Rev. B 20, 2206 (1979).